Analyst

Accepted Manuscript

ROYAL SOCIETY OF CHEMISTRY

www.rsc.org/analyst

Direct Glucose Sensing In the Physiological Range Through Plasmonic Nanoparticle Formation

Sarah Unser, Ian Campbell, Debrina Jana, Laura Sagle*

*Department of Chemistry, College of Arts and Sciences, University of Cincinnati, 301 West Clifton Court, Cincinnati OH 45221-0172

*Corresponding author. Tel: +1 513 556 1034; Fax: +1 513 556 9239. E-mail: saglela@uc.edu

Keywords: diabetes, biosensing, glucose, gold nanoparticle, colorimetric, label-free

Abstract

Development of improved glucose detection has vast significance in both clinical and point of care settings. Herein, we present a novel, label-free, enzyme-free, colorimetric method of glucose detection that relies on the reduction of a gold salt precursor facilitated by physiological concentrations of glucose (1.25 mM – 50 mM). The concentration of glucose present during the reduction process results in nanoparticles of different size, which in turn change the color of solution. Through transmission electron microscopy (TEM), it was found that the nanoparticle size decreases as the glucose concentration increases. Kinetic characterization of nanoparticle formation shows rate constants change two orders of magnitude when comparing normal versus diabetic glucose concentrations. Assay versatility was also investigated through incorporation onto solid substrates as well as the addition of a filtering step, which produced relatively clear samples below the diabetic cut-off (10 mM glucose) and colored samples above. The colorimetric sensor was then found to also show similar color changes with glucose solutions containing biological interfering agents as well as samples with 20% serum. Last, the sensor was tested in solution containing 100% mouse serum and 100% bovine urine spiked with varying glucose concentrations, which resulted in smaller nanoparticle formation whose intensities were dependent on glucose concentration. The resulting color changes observed for this sensor in urine samples are directly compared with Benedict's reagent and are shown to be significantly more sensitive to lower concentrations of glucose in the diabetic relevant range.

Introduction

Diabetes mellitus affects 382 million people worldwide, many of whom are in developing countries where issues of cost and hospital accessibility are paramount.[1] Therefore, there is a great need for accurate, quantitative, inexpensive and noninvasive glucose sensing devices. Current methods of glucose detection rely on the electrochemical detection of either hydrogen peroxide by-product or electrons released upon oxidation of glucose via the glucose oxidase enzyme.[2, 3] Although this method has yielded quantitative, accurate glucose detection, the high cost of battery-operated meters and test strips and invasive finger pricking has limited their use, particularly in developing countries. In addition, glucose detection is indirect and requires enzymatic reactions that are sensitive to heat and pH, and therefore cannot be stored for long periods of time. Recently other techniques, such as field effect transistors[4, 5] and MEMS devices,[6, 7] which show increased sensitivity and quantification, have been employed for glucose detection. Unfortunately, these techniques also rely on indirect glucose detection and often employ enzymatic reactions for detection. Moreover, fabrication and detection is time consuming and expensive, which would result in high device cost.

Colorimetric glucose detection has the advantage that changes can be detected by eye, which could lead to significantly cheaper devices. Colorimetric glucose detection has been carried out for many years with chemical dyes sensitive to glucose itself, thus capable of direct glucose sensing. Some common examples include Azo dyes[8] and catechol dyes[9], many of which are now being incorporated into hydrogels and polymers for improved device fabrication.[10, 11] In addition, tests based on the reactivity of metal salts with glucose and other reducing agents, such as the Benedict's and Tollen's reagents, have been widely employed for inexpensive, non-invasive glucose testing.[12, 13] However, issues with selectivity and quantification, particularly in

the physiological range, plague the use of many of these simple tests. Recently, plasmonic glucose sensors have been developed yielding quantitative and selective colorimetric changes. Plasmonic sensing offers advantages in yielding sensitive detection that is not susceptible to degradation, reactivity and photobleaching.[14, 15] Some examples include Concanavalin A-mediated nanoparticle aggregation,[16] peroxide-mediated nanoparticle aggregation,[17] and boronic acid-based nanoparticle sensors.[18] Unfortunately, the systems employed in these studies suffer from similar drawbacks as those mentioned above, mainly, that enzymatic reactions are often used, which are heat and pH sensitive, and/or the systems are not sensitive to physiological concentrations of glucose, which are quite high.

It has been shown that glucose is able to both reduce and cap noble metal salts for a "greener" synthesis of nanoparticles.[19, 20] Often, when the concentration of capping or reducing agent is altered, different size and/or shape nanoparticles result, which in turn produce changes in the color of solution.[21, 22] Thus, noble metal salts in solution should be sensitive to changing glucose concentration and the color of the solution should reflect this change. It should therefore be possible to make a quantitative, colorimetric glucose sensor with only a solution of dilute gold salt, see **Figure 1**.

Herein, we report a novel, enzyme-free, colorimetric method of rapidly and directly detecting glucose in the physiologically relevant range (1 mM – 50 mM) by reacting glucose with gold salt in solution. As depicted in **Figure 1**, as the glucose concentration increases from the normal to the diabetic range, the resulting plasmon resonance peak maximum shifts yielding a color change from blue to red. TEM measurements confirm that substantially larger nanoparticles are present in solutions containing lower glucose concentrations, whereas higher glucose concentrations result in smaller nanoparticles. The kinetics of nanoparticle formation fits

well to a seeded growth model and is also shown to be dependent on glucose concentration. The smaller nanoparticles formed at higher glucose concentrations form substantially faster than the larger particles at lower glucose concentrations. The versatility of this simple assay is then explored by exposing the resulting nanoparticle solutions to 0.1 μm porous filtration to produce solutions that go from clear to colored when diabetic glucose concentrations (>10 mM) are present. In addition, nanoparticle arrays on a glass substrate were treated with thiol groups to attract nanoparticles in solution to bind. After exposure of these solid substrates to nanoparticle solutions produced from different concentrations of glucose, the plasmon resonance maximum and color of the substrates changed from pink to blue, depending on the glucose present in the nanoparticle solutions. Finally, since this assay is based on simply reducing gold in solution, it was assumed that any reducing agent present in biological solutions would interfere. Therefore, the ability to detect glucose in complex biological solutions is explored. Surprisingly, nanoparticle formation and color change is shown to proceed similarly in solutions containing both glucose and other biological interfering agents. This is attributed to the fact that glucose is present in many biological fluids, such as blood, in substantially higher concentrations (1000 fold) than other reducing species. Further, samples with varying concentrations of glucose present in 20% mouse serum also produce nanoparticles of similar size and color to their pure glucose counterpart. Lastly, samples are tested in whole mouse serum and bovine urine and directly compared with the Benedict's reagent, which is commonly used to detect glucose and other reducing agents in urine. Our samples show increased sensitivity to glucose compared to Benedict's reagent, particularly in urine samples where the glucose concentrations are roughly 10 fold lower than that found in blood. Thus, the simple, rapid, inexpensive assay described herein should prove very useful for non-invasive, sensitive glucose detection in the field.

Experimental

Synthesis of Au Nanoparticles. The synthesis of gold nanoparticles using glucose as both a capping and reducing agent was carried out according to previous reports.[20, 23] All of the solutions were prepared using Milli-Q water filtration system 18.2 Ω. D-dextrose (Fisher Scientific) solutions were prepared to each respective concentration using deionized water. Glucose solutions of a given concentration were added in 500 µL aliquots to a microcentrifuge tube, and the tube was placed on a vortexer speed 2. While vortexing, 10 µL of 1 M sodium hydroxide (Fisher Scientific) was added to the glucose solution to induce alkaline pH. After approximately 10 seconds 2.0 x 10^{-4} M tetrachloroauric acid, $HAuCl_4$, (Acros) was added to the vortexing solution. After a duration of 5-70 seconds a color change occurred indicating the completion of the reaction and formation of gold colloids. Agitation by vortexing was continued for 5 – 10 seconds after color change to ensure reaction completion.

Sample Characterization. LSPR measurements were taken using 3900-Hitachi UV-visible spectrometer. The solid substrates were characterized in transmission mode using a USB-2000 Ocean Optics UV-visible spectrometer powered by an HL-2000-HP tungsten halogen lamp. Transmission electron microscopy (TEM) studies were carried out using an FEI CM- 20 at 200 eV. Additional TEM images were taken using a JEOL 1230 at 80 eV, and images were taken using an AMT Advantage Plus 2k x 2k digital camera. Samples were prepared on ultrathin carbon type-A, 400 mesh Cu grids coated with formvar (Ted Pella). Samples were prepared by diluting the samples in 50 mM HEPES buffer by half and micropipetting drop wise onto the grid surface. Excess nanoparticle solution was subsequently wicked away. The solid substrates with nanoparticle arrays were characterized using an FEI (Phillips) XL30 Field Emission Scanning

Electron Microscope. Sample preparation of SEM measurements were carried out by first drying solutions of nanoparticles in varying glucose on the glass surface and then sputtering 50 nm of gold over the arrays to prevent charging.

Real-Time Studies. Real time kinetic measurements of nanoparticle formation in solutions of varying glucose concentration were taken using a USB-2000+ Ocean Optics spectrometer with a halogen lamp. First, a quartz cuvette with a small magnetic stir bar was placed in the cell holder and the whole assembly put on top of a magnetic stir plate. Next, 500 μL of each respective glucose concentration and 10 μL of 1 M sodium hydroxide were added to a quartz cuvette. Using a syringe, 500 μL of 2 x 10^{-4} M $HAuCl_4$ was added to the cuvette, and intensity changes in a narrow wavelength range (~20 nm), depending on nanoparticle size, were monitored with time.

Measuring Color Changes of Nanoparticle Arrays on Glass. The samples used to demonstrate that the assay could be extended to a surface contain an array of 60 nm silver particles generated using Hole Mask Colloidal Lithography. These substrates were made according to recent literature reports.[24, 25] Briefly, 4% polymethylmethacrylate (PMMA) solutions in anisole (Microchem Corporation) were spin-coated (3000 rpm for 30 seconds) onto piranha-cleaned glass cover slips (No. 2). The surface of the PMMA layer was then rendered hydrophilic through 5 seconds of oxygen plasma etch, and a second polymer layer of polydiallylammonium (PDDA) was drop-coated on top of the PMMA layer. A 0.2% solution of 60 nm carboxylated polystyrene spheres (Invitrogen, Inc.) was then drop-coated on top of the polymer assembly and dried, followed by e-beam deposition of 5 nm of gold. The polystyrene spheres were then removed by tape-stripping, and the samples subjected to 2 minutes of oxygen plasma etch, which created hole-masks with 60 nm holes. A second deposition of 60 nm of silver

was then deposited onto the samples, followed by mask lift-off in acetone, leaving an array of silver nanoparticles approximately 60 nm in diameter and 60 nm high on the glass coverslips. The surface of the nanoparticle arrays were then soaked in ethanol (99% purity) and 1 x 10^{-2} M of 11-mercaptoundecanoic acid (MUA) overnight. Next, 10 mg/mL of N-Hydroxysuccinimide (NHS, Thermo Scientific) in 0.05 M 2-ethanesulfonic acid buffer (MES, Sigma Aldrich) was added to the surfaces for 10 – 15 minutes to activate the carboxylic acid groups on MUA. The samples were then rinsed with 0.05 M MES buffer and 10 mg/mL of 2-aminoethanethiol hydrochloride(Acros Organics) with 10 mg/mL of 1-Ethyl-3-(3-dimethylaminopropyl)carbodiimide (Thermo Scientific) in 0.05 M MES buffer was added to the samples for 1 hr. Last, the substrates were washed in MES buffer, next washed with deionized water, followed by ethanol and dried in nitrogen gas. Nanoparticles that have been reduced by glucose were then diluted by a third in 0.05 4-(2-hydroxyethyl)-1-piperazineethanesulfonic acid (Sigma Aldrich, HEPES buffer), pH 7, to change the pH of the nanoparticles from alkaline to neutral. The nanoparticles were then added to the surfaces containing silver nanoparticle arrays and soaked for 1 hour, followed by drying in nitrogen gas just prior to measurement.

Filtering Samples for a Change in Color Intensity. Nanoparticles were formed as described in the glucose reduction of gold salt procedure. Immediately following the formation of glucose reduced/capped gold nanoparticles, 500 µL of 50 mM HEPES pH 7 was added to the colloidal solutions to lower the pH from alkaline to neutral. UV-Visible measurements of the nanoparticles were carried out to determine the initial plasmon absorbance peak. Next, samples were taken up by a syringe and needle. The needle was removed, and the syringe was screwed into a Whatman Anotop 25 0.1 µm filter. The nanoparticle solution was then pushed through the

Whatman filter once. The final solution that was filtered was characterized for a second time by UV-visible spectroscopy.

Testing Against Interfering Agents in Vitro. A stock solution of twice the physiological concentration of fructose, galactose, ascorbic acid, glutathione and lipoic acid was prepared.[26, 27] Glucose concentrations were prepared to twice the concentration that was desired to be tested. Next, 250 μL of the stock solution of interfering agent was combined with 250 μL of glucose solution to result in a final solution that is at the desired glucose concentration and the physiological range for interfering reducing agents. While vortexing the glucose and interfering reducing agent mixture, 10 μL of 0.5 M NaOH was added to the solution. After approximately 15 seconds, 500 μL of 0.2 mM $HAuCl_4$ was added. Once a color change was visible, solutions were vortexed for an additional 10 seconds to ensure reaction completion.

Sensing in Complex Solutions. Mouse serum (Sigma/Aldrich, Inc.) was diluted to 20% serum with a concentrated glucose sample that was also diluted to its respective concentration. Next, 500 μL of 0.8 mM $HAuCl_4$ was aliquot into a microcentrifuge tube and placed on a vortexer. While vortexing, the diluted mouse serum spiked with glucose was added to the sample. Samples were vortexed for approximately 1 minute, and left on the bench until a color change developed. For rapid detection of mouse serum, 250 μL of 100% mouse serum was added to 250 μL of 0.4 mM of $HAuCl_4$. Samples were then placed in boiling water, and a color change was observed within 3 minutes.

Benedict's reagent (Ricca Chemical Company) was tested with glucose solutions by adding 50 μL of each respective glucose solution to 500 μL of Benedict's reagent.[28] The glucose-Benedict's reagent solution was then added to boiling water for approximately 3 minutes, and then removed from heat. A similar procedure was used to test for glucose in bovine

urine. Bovine urine (Lampire Biological Laboratories) was spiked with glucose at various concentrations, and was tested against Benedict's reagent by adding 50 μL of bovine urine to 500 μL of Benedict's reagent. The bovine urine-Benedict's reagent solution was then added to boiling water for approximately 3 minutes, and then removed from heat.

Tests were then conducted against the reduction assay by adding 500 μL of urine to 500 μL of 4.0 x 10^{-4} M tetrachloroauric acid and 60 μL of 1 M NaOH. The mixture was then added to boiling water for 2 minutes and 30 seconds, and then placed on ice for 5 minutes immediately after removal from the boiling water bath.

Results & Discussion

Colorimetric Sensing In Glucose Solutions. Under alkaline conditions, the aldehyde of glucose reduces $HAuCl_4$ from a +3 to zero oxidation state to form gold nanoparticle seeds in solution.[29] In addition, glucose effectively 'binds' to the gold nanoparticle surface acting as a capping agent and influences the final size of the nanoparticle produced. Indeed, visual inspection and UV-Vis spectra of the gold salt solutions at different glucose concentrations show marked changes, see **Figure 2**. At lower glucose concentrations, the solutions appear purple-blue and the plasmon resonance peak is above 550 nm. In contrast, at high glucose concentrations, the solutions appear pink and the plasmon resonance peak shifts to lower wavelengths, below 550 nm. If no glucose is present in these alkaline solutions of gold salt, no color formation appears, see **Figure S1**. When plotting the shift in plasmon resonance vs glucose concentration (see **Figure 2** inset), it is evident that the largest shifts are observed below 18 mM glucose concentrations. Healthy blood glucose concentrations less than 10 mM are considered normal, whereas those above 10 mM are abnormal, rendering this sensitivity range undoubtedly useful

for diabetes testing and maintenance.[30] In addition, nanoparticle formation and color was reproducibly observed at concentrations as low as 1.25 mM glucose. This low limit of detection is significant for testing hypoglycemia, a common condition which can lead to coma and even death. Nanoparticle formation was attempted at glucose concentrations less than 1.25 mM, but unreliable color formation resulted. Thus, the limit of detection of this colorimetric assay appears to be close to 1.25 mM glucose. In addition, no further changes in plasmon resonance are observed above ~20 mM glucose revealing 'saturation' behavior at higher glucose concentrations. One explanation for this behavior is that glucose is capping the surface of the nanoparticles that are formed in solution. Once the nanoparticles have formed, there is a finite amount of surface available to be capped. At glucose concentrations above 18 mM, the excess glucose is no longer able to interact with the nanoparticle surfaces directly, and thus, no change in nanoparticle size or shape is observed. In order to confirm that changing the concentration of glucose in solution would in turn change the size or shape of resulting nanoparticles, TEM measurements of the nanoparticle solutions were carried out. As shown in **Figure 3**, the nanoparticles formed at glucose concentrations below 10 mM are significantly larger than those formed at glucose concentrations above 10 mM glucose. The size difference between the nanoparticles at different glucose concentrations correlates nicely with the observed change in plasmon frequency, similarly reported elsewhere.[31, 32] Indeed, nanoparticles formed at different glucose concentrations (1.25-50 mM) are close to those calculated using the standard size estimation model, which yields values ranging from ~110 nm to ~10 nm.[33] The large nanoparticles formed at lower glucose concentrations are likely the result of both an aggregative kinetic mechanism (see the Avrami model below) as well as late stage Ostwald Ripening, as observed by previous reports when capping agent is a limiting factor.[22, 34, 35] **Figure S2** of the

Supplemental Section contains TEM images of samples with glucose concentrations not shown in **Figure 3**.

Next, to further investigate the differences in nanoparticle formation at low and high glucose concentrations, kinetic measurements were carried out. For all solutions, the plasmon peak of interest was monitored with time as the solutions were added together and mixed. The kinetic data at 5 different glucose concentrations was selected and is shown in a stacked plot in **Figure 4a**. This data shows a clear trend that as glucose concentration is increased, nanoparticle formation occurs much more rapidly. The solutions containing less than 3 mM glucose take in excess of 60 seconds to show color, whereas the solution with 20 mM glucose reacts in only 11 seconds. The observable trend shown in **Figure 4b** of increasing glucose concentration and decreasing nanoparticle formation time is another useful method for the quantification of glucose concentration. Slower nanoparticle formation, greater than ~25 seconds, is related to healthy blood glucose levels while faster nanoparticle formation, less than ~25 seconds, is attributed to high blood glucose levels. When plotting out the total elapsed time vs glucose concentration and overlaying it with the data shown in **Figure 2**, it is evident that the kinetic trends are correlated with the change in nanoparticle size (see **Figure 4b**). In addition, no change in kinetics is observed when comparing glucose concentrations of 15 mM and above, which argues that glucose present in excess of 15 mM does not play a direct role in nanoparticle formation. The kinetic data shown in **Figure 4a** was fit to the Avrami model for seeded growth according to the following expression[36, 37]:

$$Absorbance = C(1 - e^{-kt^n})$$

Where *C* is the proportionality constant, *k* is the apparent rate constant and *n* is the critical growth exponent. This kinetic model is widely used to describe aggregative nanoparticle growth and has been applied to the growth kinetics of systems ranging from polymers to crystals.[38, 39] The data at the majority of the glucose concentrations fit reasonably well to this model, which implies that the seeded or aggregative growth mechanism is in fact dominant.[40] However, the data at low glucose concentrations deviates somewhat from the model, particularly at the onset of the sigmoidal curve. This could be indicative of a much slower nucleation phase in the beginning, giving rise to more of a linear increase at first. Indeed, the time to generate critical aggregates in the nucleation phase appears to be effected by the lack of glucose at concentrations below 10 mM glucose. In addition, deviations towards the end of the kinetic trace (see **Figure S4**) have previously been associated with Ostwald Ripening commencing after initial nanoparticle formation, which is more prominent when the nanoparticle surfaces are not fully 'capped'.[41] This is also most prevalent at low glucose concentrations, i.e. 1.5 and 3 mM glucose samples shown in **Figure 4a**. **Table 1** below shows the parameters obtained from fitting the kinetic data to the Avrami model. At lower glucose concentrations, the rate constant is relatively small, reflective of the long time required for nanoparticle formation. At higher glucose concentrations, the rate constant increases by 5-8 orders of magnitude, also aligned with the drastic decrease in the time for nanoparticle formation, which takes place in less than 15 seconds in solutions containing 20 mM glucose. The critical growth exponent parameter is associated with the size and dimensionality of the 'critical nucleus' or seed particle required for nanoparticle formation to proceed.[42, 43] The overall large values for the critical growth exponent indicate growth is most likely not directional, random and unimpeded.

Table 1. Kinetic parameters obtained from the fits shown in Figure 5 for nanoparticle formation at different glucose concentrations.

Glucose Conc. (mM)	Rate Constant, k (sec^{-n})	Critical Growth Exponent, n
1.5	$5.9 \pm 4.7 \times 10^{-13}$	5.0 ± 0.0173
3	$3.4 \pm 0.2 \times 10^{-9}$	5.0 ± 0.005
5	$3.3 \pm 4.0 \times 10^{-7}$	4.9 ± 0.000
10	$1.9 \pm 1.8 \times 10^{-6}$	4.9 ± 0.050
20	$1.6 \pm 2.6 \times 10^{-3}$	4.4 ± 0.050
50	$8.6 \pm 1.4 \times 10^{-4}$	4.5 ± 0.100

The kinetic parameters obtained from fitting the data of all glucose concentrations tested is shown in **Table S3**.

Versatility of the Assay. For many applications, it is advantageous to have a sensor that is bound to a surface to facilitate incorporation into on-chip, microfluidic devices.[44] These on-chip devices would require significantly lower amounts of both reagent and biological fluid, leading to a less invasive and less expensive product. The cost per assay on a relatively large scale (~2 milliters) is estimated to be roughly 2 cents, and it is conceivable a microfluidic device could reduce the cost further by 100 fold. Towards this goal, we have investigated binding nanoparticles formed in solution at different glucose concentrations to a surface-bound array of silver nanoparticles. This array of silver nanoparticles was made using Hole Mask Colloidal lithography, as described in the **Materials and Methods** section. Carbodiimide chemistry was then used to couple an alkanethiol to the surface of these silver nanoparticles on glass, with a thiol group facing outward. Upon addition of the gold nanoparticle solutions, the nanoparticles in solution bind to the sulfide groups on the surface and 'bind' to the nanoparticle array, causing the surface to change color. As shown in **Figure 5**, addition of nanoparticle solutions with different

glucose concentrations to the surface-bound arrays did yield shifts in the plasmon resonance and color changes. Solid substrates soaked for the same time in buffer solutions containing no glucose did not result in color change, see **Figure S4**. It was expected that the binding of larger nanoparticles, formed at lower concentrations of glucose, would yield the largest shifts. Surprisingly, the opposite trend was observed, instead the higher concentrations of glucose showed the largest shifts in plasmon resonance and color. To further investigate this unexpected trend, SEM images were taken of the substrates treated with nanoparticle solutions containing different concentrations of glucose. Interestingly, although the solutions of higher glucose concentration (50 mM) do yield smaller nanoparticles, the amount of nanoparticles is greatly increased, giving rise to small nanoparticles observed everywhere on the glass surface. At lower glucose concentrations, the larger and fewer nanoparticles only bound in relatively small areas, producing smaller changes in color and shifts in plasmon resonance. Nevertheless, the color of the solid substrates did show a trend with glucose concentration; the low concentrations yielded the smallest color change and the high concentration the largest change in color.

Further versatility is demonstrated by filtering gold nanoparticle solutions containing different glucose concentrations through 0.1 μm pore syringe filters. It was expected that at low glucose concentrations (<10 mM) the large nanoparticles would not go through the filter and the solutions would appear more clear. Whereas, at higher glucose concentrations, the smaller nanoparticles would be able to transverse through the 100 nm pores and less of a change in color would result. Indeed, we did find this to be the case. The samples with low glucose concentrations became significantly less colored after passing through the filters, whereas the higher glucose concentrations showed little change in color intensity, see **Figure 6**. These samples were also analyzed by taking TEM images before and after filtering in solutions

containing 3 mM and 20 mM glucose, see **Figure S7**. These measurements confirm that the filters are indeed removing larger nanoparticles, >100 nm, from the solution containing 3 mM glucose, whereas the nanoparticles remain similar in size and density for the samples containing 20 mM glucose. Interestingly, samples below the diabetic cut-off (~10 mM glucose), show the most pronounced decrease in color intensity, whereas samples above this cut-off show small changes in color intensity. This fast, simple filtering step demonstrates the assay can extended to only yield color in samples containing diabetic glucose concentrations.

Colorimetric Sensing In Complex Biological Solutions. We have demonstrated the reduction of tetrachlorauric acid in the presence of glucose, however, in real biological samples there are other reducing molecules present. In serum, these reducing molecules consist of ascorbic acid, fructose, galactose, glutathione, lipoic acid and uric acid.[26] In order to compare how these reducing agents affect our colorimetric assay, nanoparticle formation was observed in solutions containing different concentrations of glucose in addition to physiological concentrations of five of the six molecules above (uric acid was not tested due to problems with sample precipitation). A plot of shift in plasmon resonance vs glucose concentration for both solutions containing only glucose and those with glucose and other reducing agents is shown in **Figure 7**. Sample containing only interfering agents, and no glucose were also tested and showed no color change in a 3 hour time span, see **Figure S1**. The samples containing other interfering agents showed larger shifts in plasmon resonance and solution color when compared to solutions containing the same concentration of only glucose. This implies that the assay is more sensitive when other reducing agents are present. This larger shift in plasmon resonance is also indicative of smaller nanoparticle formation. Confirmation of this size difference is shown in TEM images of nanoparticles formed in solutions containing 50 mM of glucose with and without other

reducing molecules, see **Figure S6**. In addition, dynamic light scattering data on samples containing 50 mM glucose with and without interfering agents also confirms that the nanoparticles are smaller in solutions containing other reducing agents, see **Figure S7**. Lastly, it is important to note that in both cases, the assay is most sensitive to glucose concentrations below 20 mM, which is the range of interest for diabetes diagnosis and maintenance.

In order to demonstrate the feasibility of this novel, simple assay in measuring real biological samples, glucose was added to solutions containing gold salt dissolved in 20% mouse serum. Although the time for nanoparticle formation was considerably slower than the in vitro samples, nanoparticle formation and color changes were observed only in the samples containing glucose, see **Figure 8**. Characterization of the nanoparticle solutions using UV-Vis spectroscopy shows the plasmon resonance frequency is very similar to that obtained for 5, 10 and 50 mM glucose solutions with interfering agents. In addition, TEM measurements reveal the size of the nanoparticles formed in samples containing 20% serum and 5, 10 and 50 mM glucose, are also closely aligned with solutions without serum, see **Figure S10**.

In order to carry out the assay in 100% mouse serum on relatively rapid timescales, samples were heated to ~100 degrees Celsius after mixing the gold salt, base, and serum samples containing glucose. Interestingly, this led to smaller nanoparticle formation as demonstrated by the orange colored samples in **Figure 7c** and the TEM data shown in **Figure S13**. Most notably, a drastic decrease in glucose sensitivity was observed; the plasmon absorption only shifted at most 10 nm when comparing the lowest and highest glucose concentrations tested. Thus, although heating the samples greatly increases the kinetics of color formation in complex biological samples, it also reduces the assay sensitivity by producing nanoparticles of similar size, and similar color, over a large range of glucose concentrations. However, it is possible to

discern differences in intensity and color of the samples as the glucose concentration is raised. The sample containing 10 mM glucose appears noticeably different in color than the sample with little or no glucose present.

Efforts to extend this inexpensive, rapid assay to applications in the field, resulted in testing urine rather than serum. The presence of glucose in the urine (greater than 1.25 mM) is not only associated with Diabetes, but ailments such as thyrotoxicosis and Cushing's syndrome.[45] Similar to the samples in serum, the urine samples were heated to induce nanoparticle formation on a relatively rapid timescale. The color and nanoparticles formed in the resulting solutions were similar to those observed in 100% serum samples, see **Figure 9a** and **Figure S14**. Interestingly, unlike samples in aqueous solution, samples in complex biological media containing no glucose were still able to yield nanoparticle formation, especially the samples in urine. Recent studies have shown that amines can efficiently form small gold nanoparticles of narrow size distribution, particularly at high temperatures.[46, 47] Since urea does contain amine compounds, it is conceivable these species are playing a direct role in nanoparticle formation. In addition, gold nanoparticles have been synthesized utilizing biological agents such as algae, bacteria and fungi.[48-50] These protocols also often use heat and produce nanoparticles similar in size to what we have observed. It is clear the mechanism of nanoparticle formation is quite different in complex biological solutions and we envision future studies aimed at better understanding these effects.

The samples tested in urine showed a marked change in color intensity as the glucose concentration was increased. A plot of plasmon intensity vs glucose concentration for these samples in urine reveal that the sample containing 3 mM glucose shows a clear increase in intensity when compared to the sample containing no glucose. The same glucose-spiked urine

solutions were tested with the Benedict's reagent, which involves copper ion reduction and precipitation. These samples showed less discernable changes in color or intensity at glucose concentrations lower than 20 mM, see **Figure 9a**. A comparison of the assay and Benedict's reagent in aqueous solutions containing different concentrations of glucose is also shown in **Figure 9**. Once again, the Benedict's reagent appears to be significantly less sensitive to solutions with lower concentrations of glucose, showing a slight color change at ~10 mM glucose. In contrast, the assay presented herein shows significant color changes in solutions containing glucose concentrations as low as 1.5 mM.

Conclusions

We have developed a novel, inexpensive, rapid, enzyme-free, colorimetric glucose detection assay sensitive to physiological concentrations of glucose, 1.25-20 mM. This assay is based on the principle that glucose can act as both a reducing and capping agent for gold nanoparticle formation in aqueous solution. At glucose concentrations below the diabetic range (<10 mM), large nanoparticles are formed, which produce blue-colored solutions. At glucose concentrations typical in diabetic patients (>10 mM glucose) significantly smaller nanoparticles result, producing pink-colored solutions. Due to the simple nature of the assay, we envision its facile incorporation into on-chip microfluidic devices in which color is produced on a solid substrate only in cases where the glucose concentration is above healthy levels. Lastly, glucose testing was carried out in biological fluids such as serum and urine and compared to the commonly used Benedict's reagent. Particularly in urine, this assay proved to be significantly more sensitive to lower concentrations of glucose and was able to detect only 3 mM glucose in

urine. Since glucose concentrations in urine are significantly less than that in serum, this assay could prove useful in detecting glucose and other reducing agents in a non-invasive manner.

Supporting Information. Detailed information depicting data not shown in figures contained in the paper is available free of charge via the Internet at *www.rsc.org/**analyst***.

Acknowledgment. This work was supported by University of Cincinnati start-up funds.

References

1. I. D. Federation, ed. T. N. Leonor Guariguata, Jessica, Beagley, Ute Linnekamp, Olivier Jacqmain, International Diabetes Federation, www.idf.org, 2013.
2. J. Wang, *Chem. Rev.*, 2008, **108**, 814-825.
3. A. Heller and B. Feldman, *Chem. Rev.*, 2008, **108**, 2482-2505.
4. K. Besteman, J. O. Lee, F. G. M. Wiertz, H. A. Heering and C. Dekker, *Nano Lett.*, 2003, **3**, 727-730.
5. A. B. Kharitonov, M. Zayats, A. Lichtenstein, E. Katz and I. Willner, *Sensor Actuat. B-Chem*, 2000, **70**, 222-231.
6. X. Huang, S. Q. Li, J. S. Schultz, Q. Wang and Q. Lin, *Sensor Actuat. B-Chem*, 2009, **140**, 603-609.
7. A. C. R. Grayson, R. S. Shawgo, A. M. Johnson, N. T. Flynn, Y. W. Li, M. J. Cima and R. Langer, *PLEEE*, 2004, **92**, 6-21.
8. N. DiCesare and J. R. Lakowicz, *Org. Lett.*, 2001, **3**, 3891-3893.
9. G. Springsteen and B. H. Wang, *Chem. Commun.*, 2001, 1608-1609.
10. X. Wu, Z. Li, X. X. Chen, J. S. Fossey, T. D. James and Y. B. Jiang, *Chem. Soc. Rev.*, 2013, **42**, 8032-8048.
11. S. Hajizadeh, A. E. Ivanov, M. Jahanshahi, M. H. Sanati, N. V. Zhuravleva, L. I. Mikhalovska and I. Y. Galaev, *React. Funct. Polym.*, 2008, **68**, 1625-1635.
12. S. R. Benedict, *J. Biol. Chem.*, 1909, **5**, 485-487.
13. G. Svehla, Vogel, Arthur Anton, *Vogel's qualitative inorganic analysis*, Longman, New York, New York, 1996.
14. L. B. Sagle, L. K. Ruvuna, J. A. Ruemmele and R. P. Van Duyne, *Nanomedicine*, 2011, **6**, 1447-1462.
15. A. G. Brolo, *Nat. Photonics*, 2012, **6**, 709-713.
16. K. Aslan, J. R. Lakowicz and C. D. Geddes, *Anal.Biochem.*, 2004, **330**, 145-155.
17. Y. Jiang, H. Zhao, Y. Q. Lin, N. N. Zhu, Y. R. Ma and L. Q. Mao, *Angew. Chem. Int. Edit.*, 2010, **49**, 4800-4804.
18. A. Pandya, P. G. Sutariya and S. K. Menon, *Analyst*, 2013, **138**, 2483-2490.
19. P. Raveendran, J. Fu and S. L. Wallen, *Green Chem.*, 2006, **8**, 34-38.

20. P. Raveendran, J. Fu and S. L. Wallen, *J. Am. Chem. Soc.*, 2003, **125**, 13940-13941.
21. D. V. Leff, P. C. Ohara, J. R. Heath and W. M. Gelbart, *J. Phys. Chem.*, 1995, **99**, 7036-7041.
22. A. Henglein and M. Giersig, *J. Phys. Chem. B*, 1999, **103**, 9533-9539.
23. G. W. Qin, J. Liu, T. Balaji, X. N. Xu, H. Matsunaga, Y. Hakuta, L. Zuo and P. Raveendran, *J. Phys. Chem. C*, 2008, **112**, 10352-10358.
24. H. Fredriksson, Y. Alaverdyan, A. Dmitriev, C. Langhammer, D. S. Sutherland, M. Zaech and B. Kasemo, *Adv. Mater.*, 2007, **19**, 4297-5002.
25. S. Cataldo, J. Zhao, F. Neubrech, B. Frank, C. J. Zhang, P. V. Braun and H. Giessen, *ACS Nano*, 2012, **6**, 979-985.
26. N. Psychogios, D. D. Hau, J. Peng, A. C. Guo, R. Mandal, S. Bouatra, I. Sinelnikov, R. Krishnamurthy, R. Eisner, B. Gautam, N. Young, J. G. Xia, C. Knox, E. Dong, P. Huang, Z. Hollander, T. L. Pedersen, S. R. Smith, F. Bamforth, R. Greiner, B. McManus, J. W. Newman, T. Goodfriend and D. S. Wishart, *PLOS One*, 2011, **6**.
27. D. S. Wishart, T. Jewison, A. C. Guo, M. Wilson, C. Knox, Y. F. Liu, Y. Djoumbou, R. Mandal, F. Aziat, E. Dong, S. Bouatra, I. Sinelnikov, D. Arndt, J. G. Xia, P. Liu, F. Yallou, T. Bjorndahl, R. Perez-Pineiro, R. Eisner, F. Allen, V. Neveu, R. Greiner and A. Scalbert, *Nucleic Acids Res.*, 2013, **41**, D801-D807.
28. About Diabetes Information: Diabetes Urine Test -- Benedict's Test, 2014.
29. C. Engelbrekt, K. H. Sorensen, J. D. Zhang, A. C. Welinder, P. S. Jensen and J. Ulstrup, *J. Mater. Chem.*, 2009, **19**, 7839-7847.
30. American Diabetes Association, www.diabetes.org, 2014.
31. J. Doak, R. K. Gupta, K. Manivannan, K. Ghosh and P. K. Kahol, *Physica E*, 2010, **42**, 1605-1609.
32. X. O. Liu, M. Atwater, J. H. Wang and Q. Huo, *Colloid Surface B*, 2007, **58**, 3-7.
33. W. Haiss, N. T. K. Thanh, J. Aveyard and D. G. Fernig, *Anal. Chem.*, 2007, **79**, 4215-4221.
34. N. T. K. Thanh, N. Maclean and S. Mahiddine, *Chem. Rev.*, 2014, **114**, 7610-7630.
35. A. K. Singh, V. Viswanath and V. C. Janu, *J. Lumin.*, 2009, **129**, 874-878.
36. M. J. Avrami, *J. Chem. Phys.*, 1940, **8**.
37. P. N. Njoki, J. Luo, M. M. Kamundi, S. Lim and C. J. Zhong, *Langmuir*, 2010, **26**, 13622-13629.
38. M. M. Despotopoulou, C. W. Frank, R. D. Miller and J. F. Rabolt, *Macromolecules*, 1996, **29**, 5797-5804.
39. E. D. Dill, J. C. W. Folmer and J. D. Martin, *Chem. Mater.*, 2013, **25**, 3941-3951.
40. S. P. Shields, V. N. Richards and W. E. Buhro, *Chem. Mater.*, 2010, **22**, 3212-3225.
41. *Controled Nanofabrication: Advances And Applications*, Pan Stanford Publishing Pte. Ltd., Singapore, China, 2013.
42. A. A. Burbelko, E. Fras and W. Kapturkiewicz, *Mat. Sci. Eng. A-Struct.*, 2005, **413**, 429-434.
43. M. J. Avrami, *J. Chem. Phys.*, 1941, **9**, 177-184.
44. B. Kuswandi, Nuriman, J. Huskens and W. Verboom, *Anal. Chim. Acta*, 2007, **601**, 141-155.
45. T. E. Murphy, Jr., *J. Insur. Medicine*, 2004, **36**, 320-326.
46. M. Yamamoto, Y. Kashiwagi and M. Nakamoto, *Z. Naturforsch B*, 2009, **64**, 1305-1311.
47. X. M. Lu, H. Y. Tnan, B. A. Korgel and Y. N. Xia, *Chem.-Eur. J.*, 2008, **14**, 1584-1591.
48. L. Castro, M. L. Blazquez, J. A. Munoz, F. Gonzalez and A. Ballester, *Let. Nanobiotechnol.*, 2013, **7**, 109-116.
49. M. E. Castro, L. Cottet and A. Castillo, *Mater. Lett.*, 2014, **115**, 42-44.
50. F. Cai, J. Li, J. S. Sun and Y. L. Ji, *Chem. Eng. J.*, 2011, **175**, 70-75.

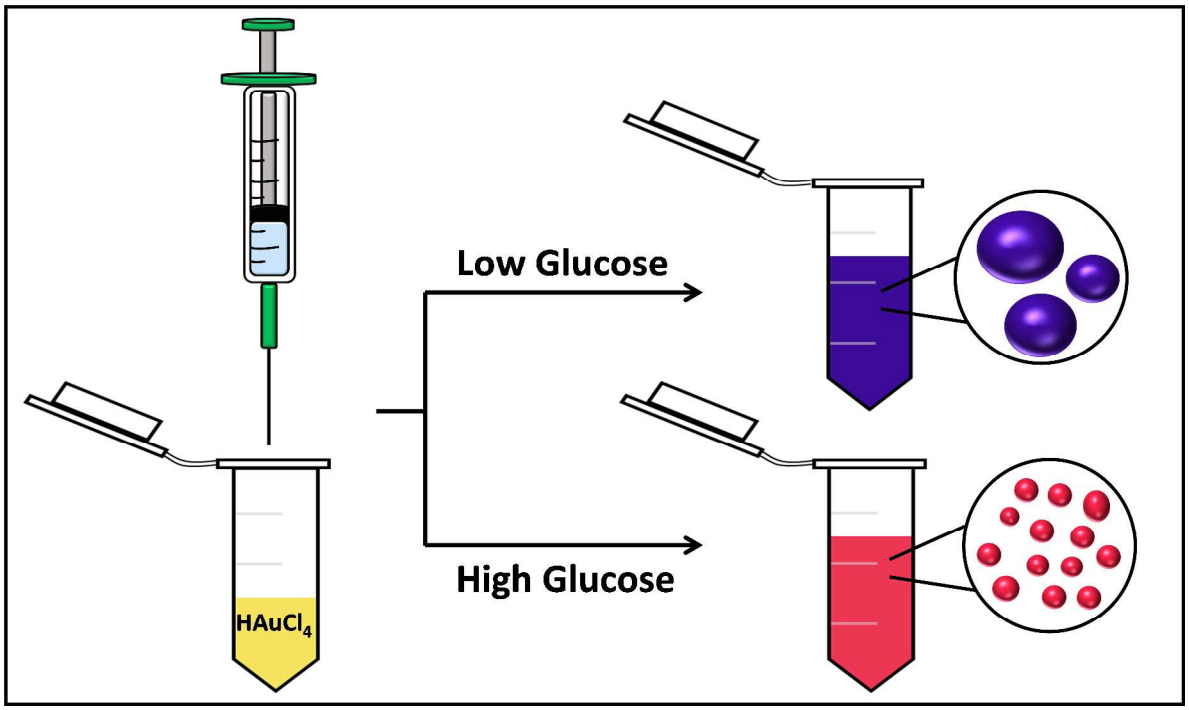

Figure 1. Depiction of plasmonic colorimetric glucose sensor in which the glucose reduces the metal salt, forming nanoparticles in solution. The size and shape of the formed nanoparticles, which determine the color of the solution, depend on the glucose concentration.

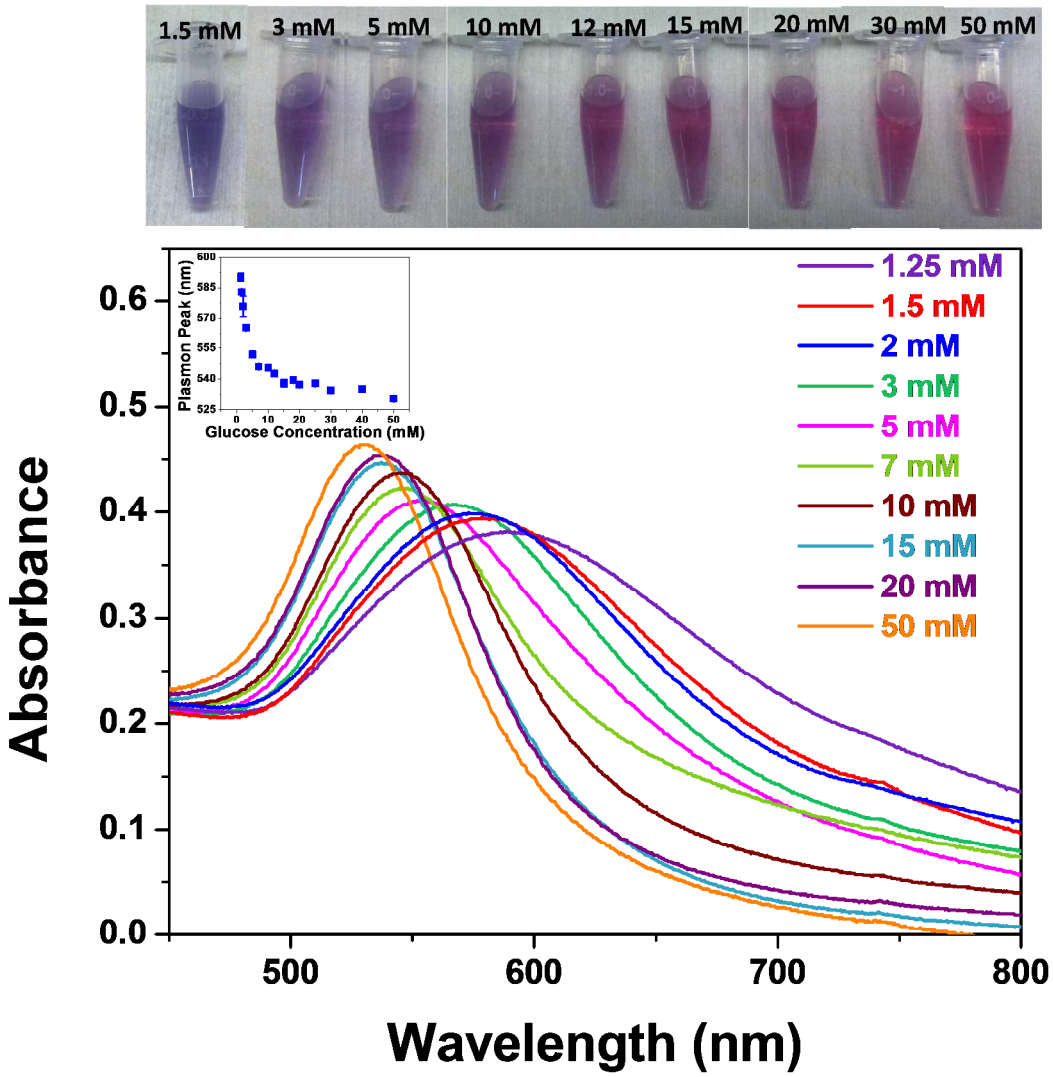

Figure 2. Changes in the localized surface plasmon resonance (LSPR) peak associated with the nanoparticles in solution at different glucose concentrations, with the trend in LSPR peak vs glucose concentration shown as an inset. Actual solutions containing gold salt and glucose at different concentrations (top).

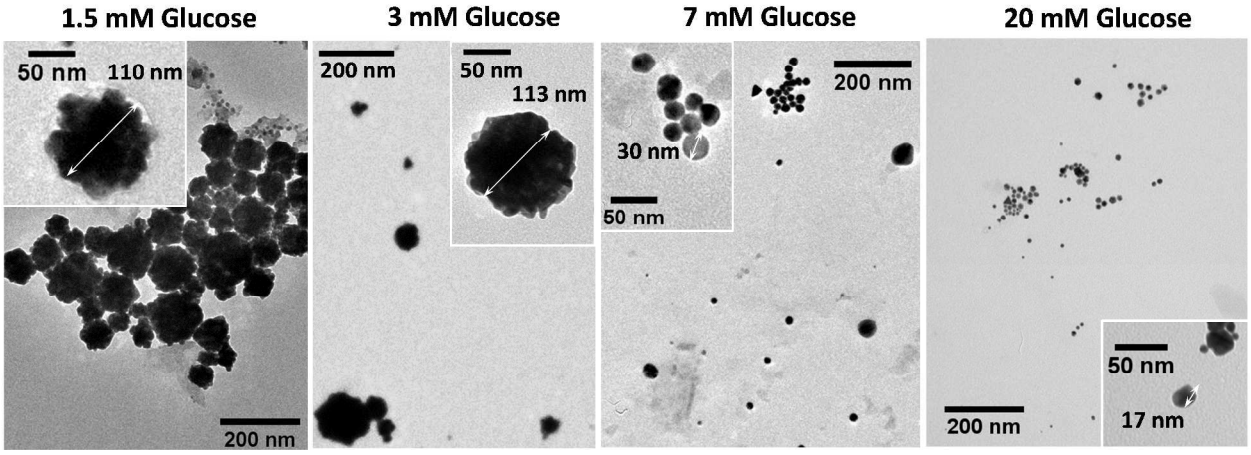

Figure 3. TEM data for nanoparticles formed at different glucose concentrations: 1.5 mM, 3 mM, 7 mM, and 20 mM glucose. As the glucose concentration is increased, smaller nanoparticles are formed in solution.

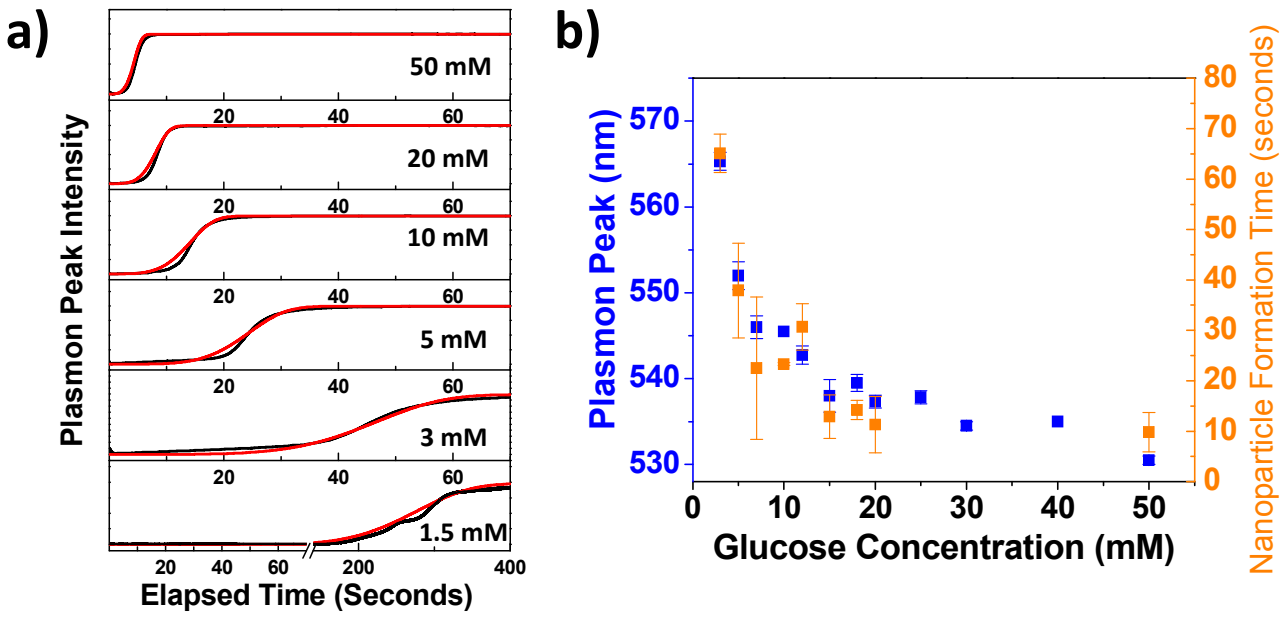

Figure 4. Plot of the intensity of a narrow wavelength range in the visible spectrum (~20 nm) vs time, indicative of nanoparticle formation, at different glucose concentrations (a). The observed trend of the kinetics of nanoparticle formation vs glucose concentration is very similar to that observed for the plasmon shift vs glucose concentration (b).

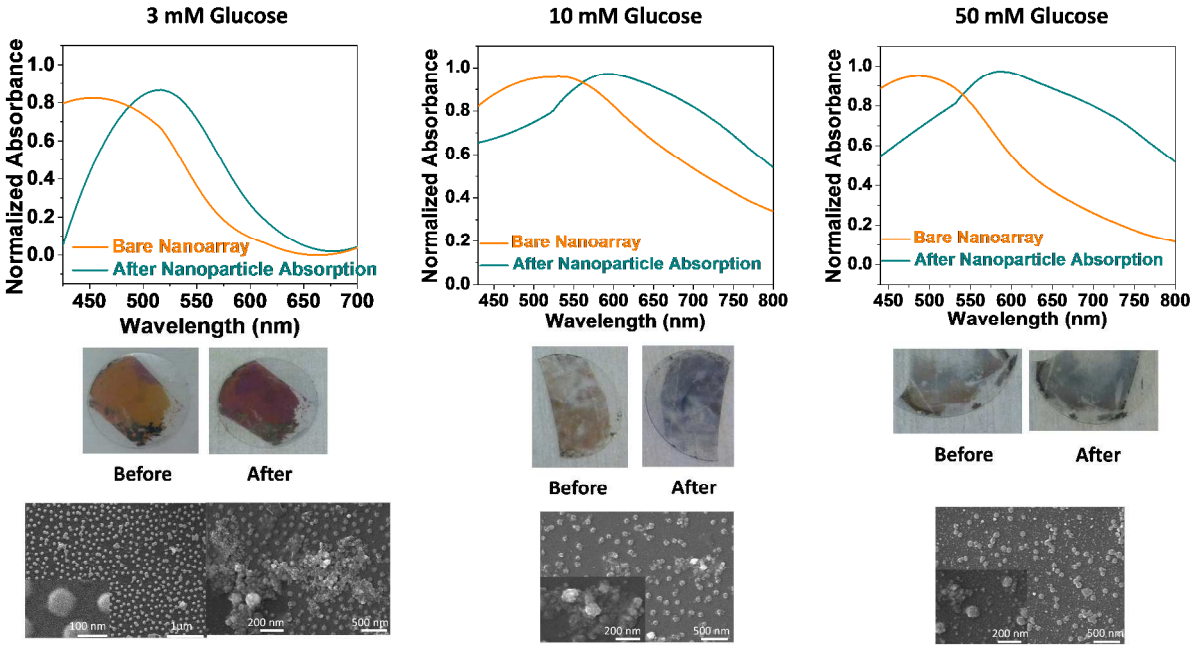

Figure 5. Adaptation of the glucose sensor to solid substrates. The nanoparticle solutions containing glucose were added to an array of 60 nm silver nanoparticles functionalized with a thiol linker to induce binding. The glucose concentrations tested were 3 mM (left), 10 mM (center), and 50 mM (right). The binding of nanoparticles in solution to this array yielded color changes, due to a change in the LSPR peak which can be detected by the naked eye. SEM measurements reveal that higher concentrations of glucose have larger amounts of small nanoparticles in solution which deposit more effectively on the surfaces, causing a greater change in color.

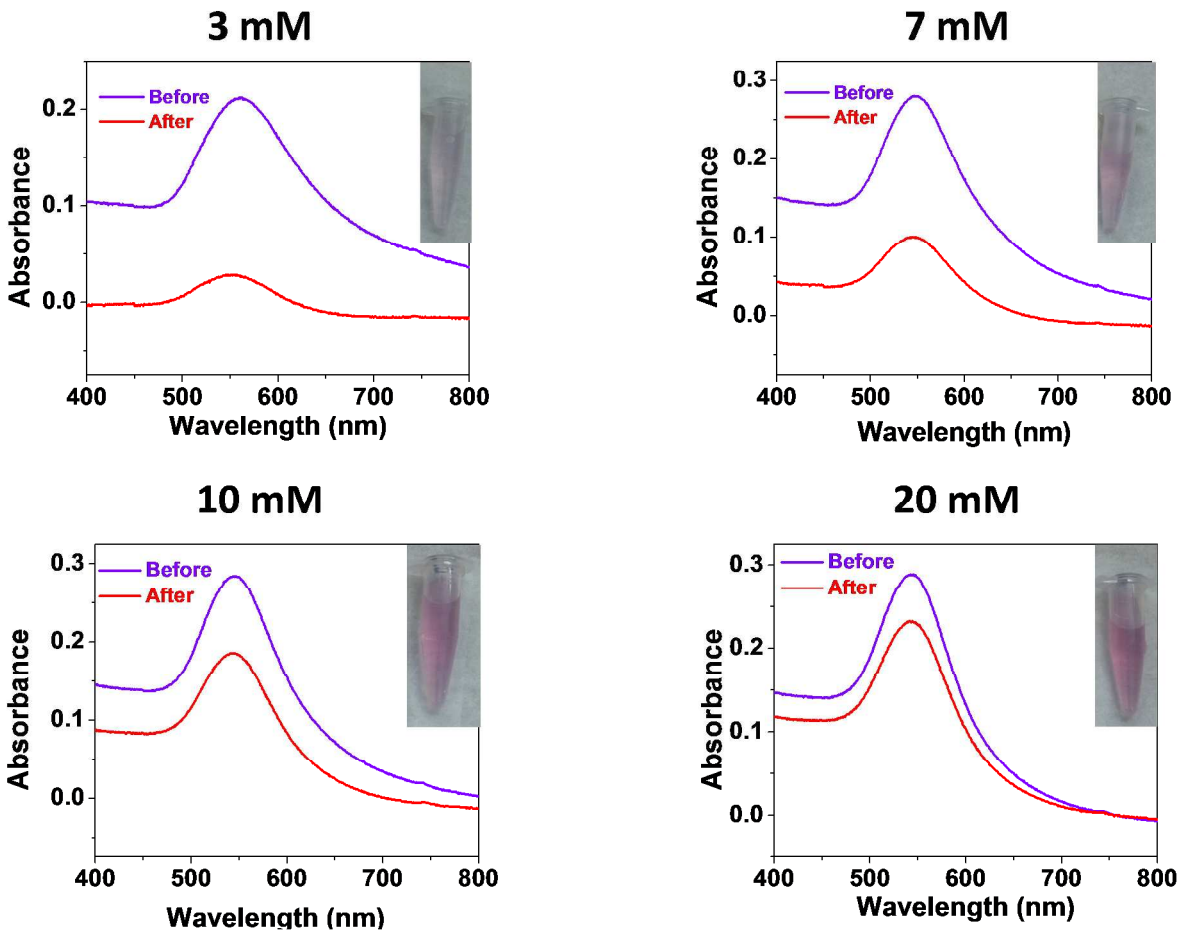

Figure 6. In order to simplify detection, the assay can be changed to produce colored solutions only at Diabetic glucose concentrations. Solutions containing various glucose concentrations, 3 mM, 7 mM, 10 mM, and 20 mM, were passed through a 0.1 μm syringe filter to generate relatively clear solutions below 10 mM glucose.

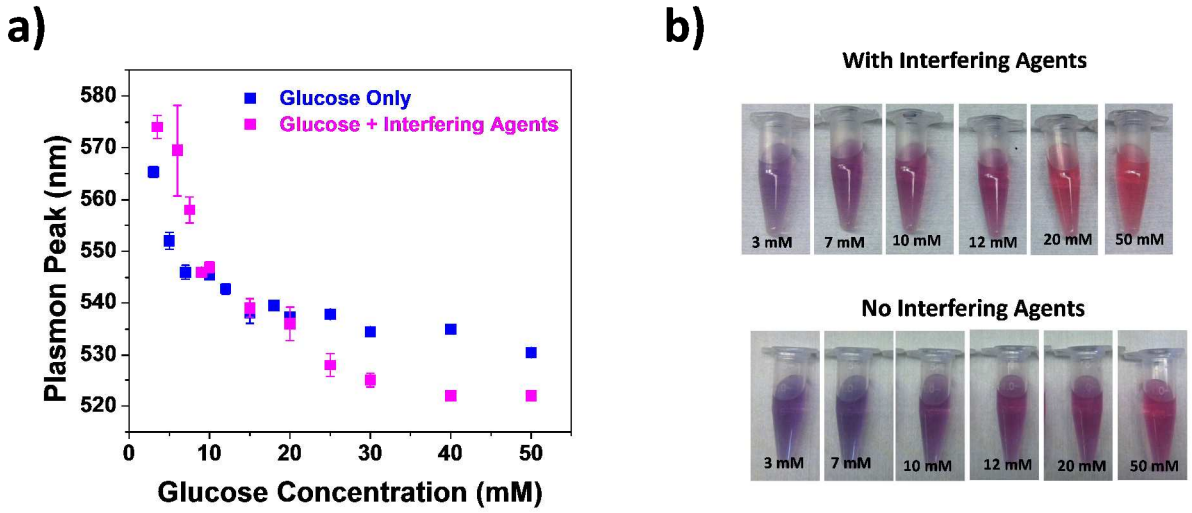

Figure 7. Comparison of the colorimetric glucose sensor with and without interfering agents. Although the overall trend of LSPR shift vs glucose concentration is similar, the total shift and steepness of the curves differ, yielding a larger dynamic range for the samples with interfering agents (a). This difference in LSPR shifts with interfering agents is evident when comparing the color of the solutions (b).

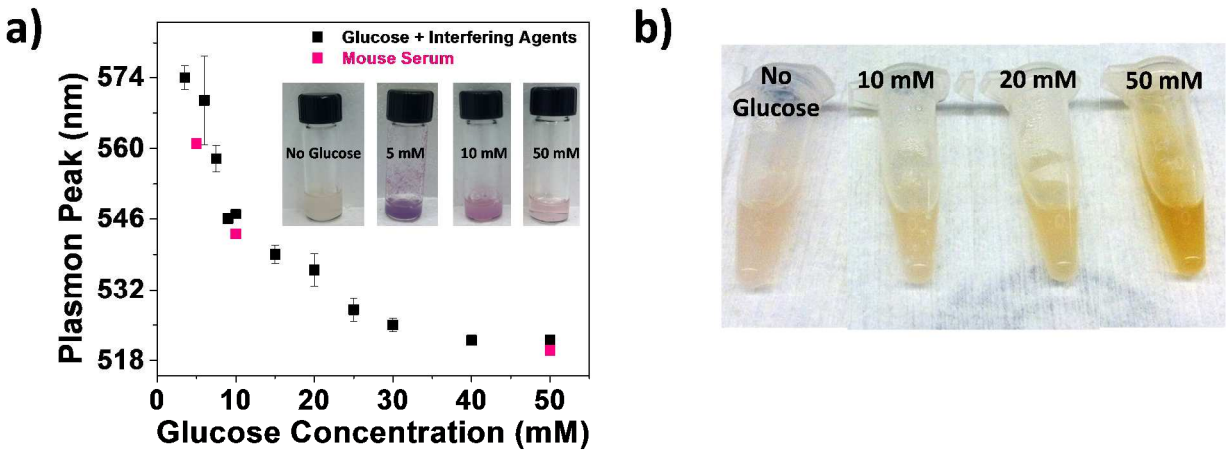

Figure 8. Investigation of the colorimetric glucose sensor in mouse serum. Nanoparticle formation in 20% serum show a correlation with data collected in aqueous solution containing interfering agent, (a). Glucose detection can also be carried out in 100% mouse serum by heating the samples at 100 °C for 3 minutes, (b).

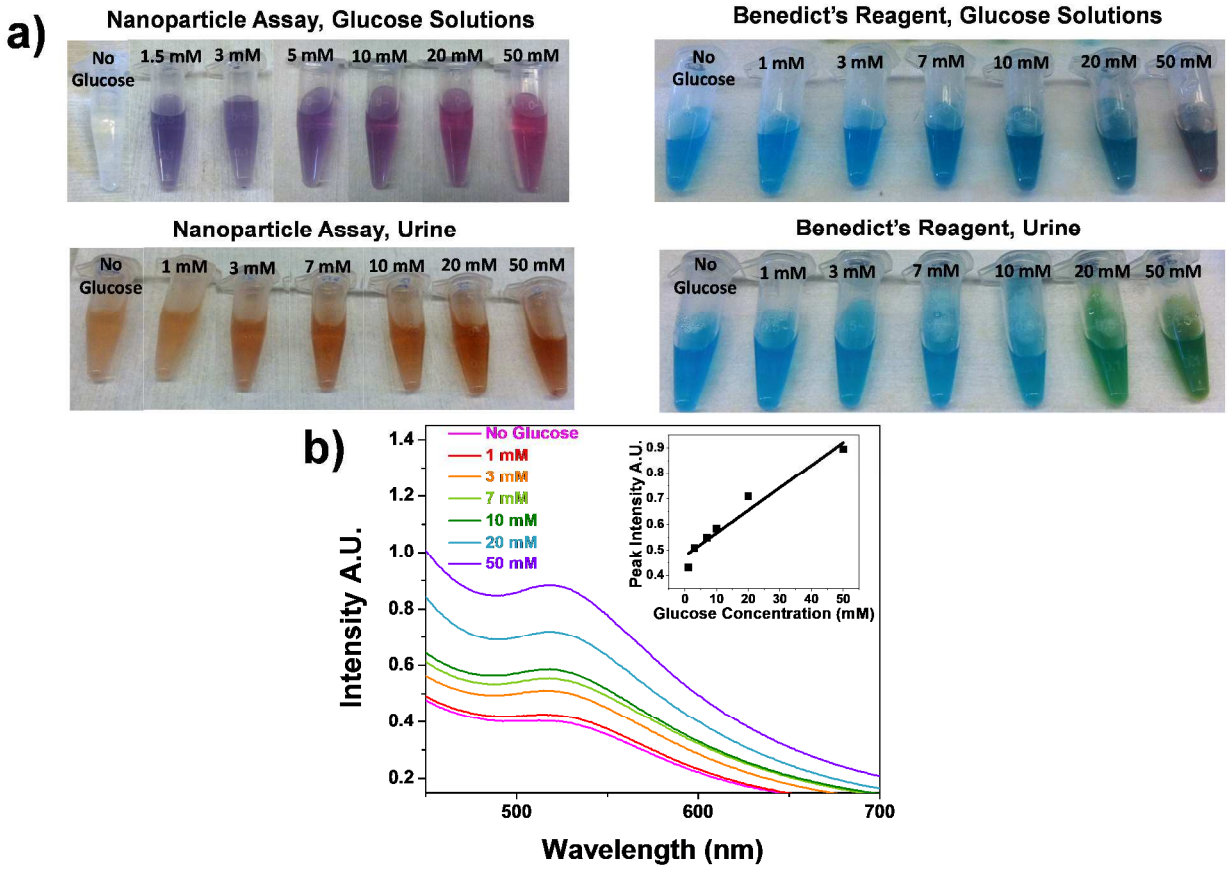

Figure 9. Comparison of the nanoparticle-based assay with the commonly used Benedict's Reagent in both glucose solutions and 100% bovine urine (a). Plot of the UV-Vis spectra of the nanoparticle assay conducted in 100% bovine urine shows a linear trend correlating to glucose concentration (b).

TOC Figure:

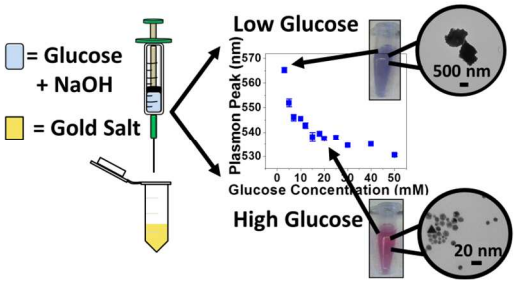

An enzyme-free, non-invasive glucose assay is developed involving gold nanoparticle formation and shows glucose sensitivity in the range of 3-50 mM in urine.